

Wigner flow reveals non-classical features of quantum phase space dynamics

Ole Steuernagel, Dimitris Kakofengitis and Georg Ritter

*School of Physics, Astronomy and Mathematics, University of Hertfordshire, Hatfield, AL10 9AB, UK**

(Dated: August 16, 2012)

The behaviour of classical mechanical systems is characterised by their phase portraits, the collections of their trajectories. Heisenberg's uncertainty principle precludes the existence of sharply defined trajectories, which is why traditionally only the time evolution of wave functions is studied in quantum dynamics. These studies are quite insensitive to the underlying structure of quantum phase space dynamics. We identify the flow that is the quantum analog of classical particle flow along phase portrait lines. It reveals hidden features of quantum dynamics and extra complexity. Being constrained by conserved flow winding numbers, it also introduces topological order into quantum dynamics.

PACS numbers: 03.65.-w, 03.65.Ta

Phase portraits characterise the time evolution of dynamical systems and are widely used in classical mechanics [1]. For the conservative motion of a single particle, moving in one dimension x under the influence of a static smooth potential $V(x)$ only, flow stagnation points determine the topology of the overall classical Liouville flow in phase space [2] and are therefore of special interest. Situated on the x -axis wherever the potential is force-free (momentum $p = 0$ and $-\partial V/\partial x = 0$), the local flow forms clockwise vortices around stagnation points at minima of the potential, maxima split the flow and therefore lie at the intersections of flow separatrices, saddle points of the potential lead to an elongated saddle flow pattern oriented along the x -axis.

A single quantum particle, free to move in time t on a line parametrised by position x is described by a complex time-dependent amplitude function $\psi(x; t)$. Wigner's function $W(x, p; t)$ [3, 4], with p the particle's momentum, is the quantum analog of classical phase space probability distributions. Structurally, W is a Fourier-transform of the off-diagonal coherences of the quantum system's density matrix ϱ , i.e.

$$W(x, p; t) = \frac{1}{\pi\hbar} \int_{-\infty}^{\infty} dy \varrho(x+y, x-y; t) \cdot e^{\frac{2i}{\hbar}py}, \quad (1)$$

with Planck's constant $\hbar = h/(2\pi)$. Unlike ψ or ϱ , the Wigner function only assumes real values, but these do become negative [3, 5], defying description in terms of classical probability theory [5], thus revealing the quantum nature of a system [5–7].

For a single quantum particle, with mass m , moving in one dimension, the time evolution of W cast in the form of a flow field $\mathbf{J}(x, p; t)$ [8], the 'Wigner flow' [9], has the two components

$$\mathbf{J} = \begin{pmatrix} J_x \\ J_p \end{pmatrix} = \begin{pmatrix} \frac{p}{m} W(x, p; t) \\ - \sum_{l=0}^{\infty} \frac{(i\hbar/2)^{2l}}{(2l+1)!} \frac{\partial^{2l} W(x, p; t)}{\partial p^{2l}} \frac{\partial^{2l+1} V(x)}{\partial x^{2l+1}} \end{pmatrix}, \quad (2)$$

fulfilling Schrödinger's equation which takes the form of the continuity equation $\frac{\partial W}{\partial t} + \frac{\partial J_x}{\partial x} + \frac{\partial J_p}{\partial p} = 0$ [3].

Wigner flow has so far not been studied in detail [8–11].

The dynamics of the harmonic potential, the most studied quantum case, e.g. of quantum optics [5, 7], amounts to a rigid rotation of the Wigner function around the origin of phase space. Only at the origin can a flow vortex form (Fig. 3 in Ref.[9]), just like in the classical case. The quantum harmonic oscillator and its isomorphism [12], the free quantum particle [13], constitute exceptional, degenerate cases where lines of stagnation of Wigner flow occur, and not only isolated stagnation points. This is due to the fact that for $V \propto x^2$ or $V = \text{const.}$ we have in eq. (2) $J_p = -W \frac{\partial V}{\partial x}$, just as in the 'classical limit' ($\hbar \rightarrow 0$) and consequently with $W = 0$ we always find $|\mathbf{J}| = 0$. Because of these three facts (rigid rotation, classical form of J_p and line formation) the non-classical phase space features discussed here cannot be seen in the degenerate cases primarily studied so far [5, 7, 13].

Here we investigate the quantum dynamics of bound states of non-harmonic potentials, their classical counterparts exhibit regular flow [2], while their Wigner flow reveals rich non-classical features:

Dependence of flow on the state of the system [14] leading to flow reversal [15] and directional deviation from classical trajectories [9], time-dependent quantum-displacement of classical stagnation points, occurrence of additional non-classical stagnation points and their dynamics (even for conservative systems), and conservation of the flow orientation winding number ω , see eq. (3) below, carried by all Wigner flow stagnation points during all stages of their time evolution—including instances when they split from or merge with other stagnation points.

The degeneracies of the degenerate cases leading to the formation of stagnation lines are lifted for non-harmonic potentials by the presence of terms with $l > 0$ in J_p and leads to the formation of separate stagnation points instead. The boundedness and continuity of wave functions of infinitely differentiable non-harmonic potentials and the unitarity of such systems' quantum dynamics induces

* O.Steuernagel@herts.ac.uk

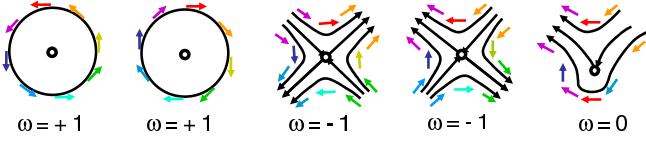


FIG. 1. (color online) Flow field around typical types of stagnation points of Wigner flow with associated winding numbers. This list is non-exhaustive.

homotopies that keep all smooth changes of \mathbf{J} in space and time around stagnation points smooth. We therefore expect that the topological structure of the Wigner flow field around stagnation points remains conserved. To monitor this we introduce the Wigner flow orientation winding number determined by the integral

$$\omega(\mathcal{L}; t) = \frac{1}{2\pi} \oint_{\mathcal{L}} d\varphi \quad (3)$$

along a closed (convex) loop \mathcal{L} ; here φ is the orientation angle between the positive x -axis and the Wigner flow ‘vectors’ \mathbf{J} . For ‘empty’ paths, not including a stagnation point of \mathbf{J} , $\omega = 0$; for vortices $\omega = +1$, see Fig 1. $\omega(\mathcal{L}; t)$ is unchanged under continuous path deformations that do not push \mathcal{L} across a stagnation point and as long as time evolution does not move a stagnation point across the loop. The winding number ω assumes integer values only (assuming the integration path \mathcal{L} does not run through a stagnation point) and is conserved. The sum of winding numbers of all stagnation points within a loop is conserved, even when they split or coalesce: the stagnation points carry topological charge [16].

To give an example, we concentrate on Caticha’s [17] smooth, slightly asymmetric, double well potential

$$\begin{aligned} V(x) = & 1 + E_0 + \frac{3}{2}\Delta E - \Delta E \alpha \sinh(2x) \\ & + \cosh^2(x) \left(\frac{\Delta E^2}{4} \alpha \sinh(2x) - \frac{\Delta E^2}{4} - 2\Delta E \right) \\ & + \frac{\Delta E^2}{4} (\alpha^2 + 1) \cosh^4(x), \end{aligned} \quad (4)$$

featuring high outer walls, and wells separated by a barrier of sufficient height, such that at least ground and first excited energy eigenstate tunnel through it, Fig. 2(a) inset. To display all non-classical flow features listed above it suffices to investigate the balanced superposition

$$\Psi(x; t) = \frac{\psi_0(x)e^{-iE_0t/\hbar} - \psi_1(x)e^{-i(E_0+\Delta E)t/\hbar}}{\sqrt{2}}, \quad (5)$$

of ground $\psi_0(x) = \psi_0 \cosh(x) \exp \left[-\frac{\Delta E}{4} (\cosh^2(x) + \alpha x + \frac{\alpha}{2} \sinh(2x)) \right]$ and first excited state $\psi_1(x) = \psi_1 [\alpha + \tanh(x)] \psi_0(x)$, with energies E_0 and $E_0 + \Delta E$ and normalisation constants ψ_0 and ψ_1 , respectively [17]. The Wigner functions have to be determined numerically [18]. Of the low energy states Ψ is the ‘most dynamic’ in that it shifts all of the particle’s probability

distribution back and forth between left and right well. Its Wigner function $W(t = T/4)$ at a quarter of the tunnelling period time ($T = 2\pi\hbar/\Delta E$) is displayed in Figs. 2 and 3.

The Wigner flow’s state dependence has two aspects: the negativity of W reverses the flow, and the dependence of J_p on W and V leads to sideways deviation of Wigner flow from classical phase portrait lines. In the case of eigenstates of the harmonic oscillator, the former leads to shear flow between neighbouring sectors of alternating polarity [9]. The latter deviation can remain mild for eigenstates of a weakly anharmonic potential [9], in our case it is very pronounced leading to the formation of non-classical vortices which are quantum-displaced off the x -axis and some of which spin anti-clockwise, Figs. 1 and 3. Indications of non-classical vortices seem to have been observed in ‘chaotic’ quantum systems before [19].

Flow reversal affects quantum tunnelling. The wave function of a particle, tunnelling through a barrier, is coherent across it, implying that interference fringes of the Wigner function form in the tunnelling region; orientated parallel to the x -axis [6], Figs. 2(b) and 3. Neighbouring phase space regions contain strips of alternating Wigner function polarity alternating their flow direction, Fig. 2(b). The further apart the two wells, all else being equal, the finer the interference pattern [6]

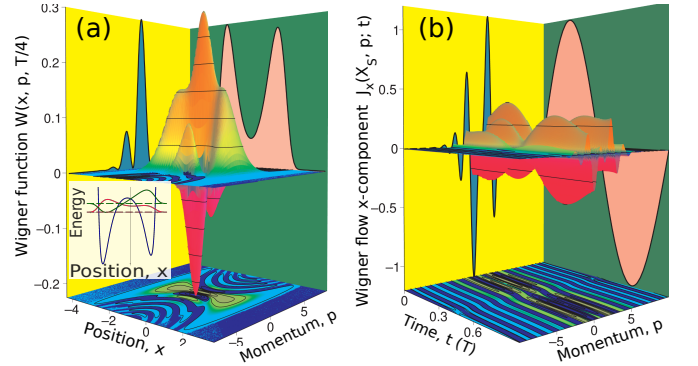


FIG. 2. (color online) Wigner function, Wigner flow and momentum distribution of state Ψ (parameters $\hbar = 1, m = 1/2, \alpha = 0.5, \Delta E = 0.5$). (a) Wigner function $W(x, p; T/4)$, projection to bottom shows its contours. Projections onto background walls show momentum and position probability distribution (blue and rose filled curves, respectively, in arbitrary units). Inset: Plot of Caticha-potential with wave functions for lowest two energy eigenstates shifted to their respective energy levels (dashed lines). (b) x -component of Wigner flow $J_x(X_S, p; t)$ at barrier top at position X_S ; bottom projection shows its contours (note its phase shift at $t = T/2$). Projections onto background walls show time and momentum projections (blue and rose filled curves, $\langle J_x(p) \rangle_t = \int_0^T d\tau J_x(X_S, p; \tau)$ and $\langle J_x(t) \rangle_p = \int_{-\infty}^{\infty} dp J_x(X_S, p; t)$, respectively, in arbitrary units). $\langle J_x(t) \rangle_p$ equals the probability current $\frac{\hbar}{2im} (\Psi^* \partial_x \Psi - \Psi \partial_x \Psi^*)$ at X_S and features the sinusoidal variation $\propto \sin(2\pi t/T)$ expected of the tunnelling current of a 2-state system.

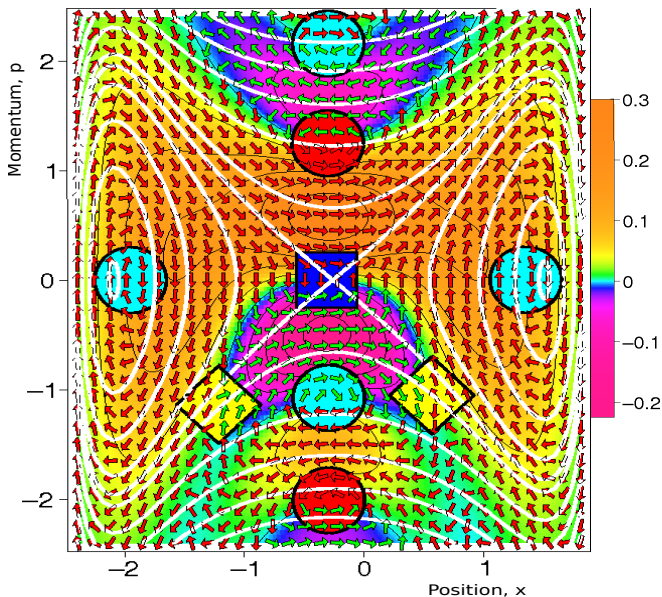


FIG. 3. (color online) Features of Wigner flow of an asymmetric double well potential (same parameters as in Fig. 1, at $t = T/4$). Colour-coded contour plot of Wigner function $W(x, p; T/4)$ (black contour lines) with an overlay of coloured arrows showing normalised Wigner flow $\mathbf{J}/|\mathbf{J}|$ (red arrows for $W > 0$ and green for $W < 0$). The classical phase portrait is shown as a collection of thick white lines. All locations of Wigner flow stagnation points are highlighted by symbols (cyan and red circles centre on clockwise and anti-clockwise vortices, respectively, yellow diamonds on separatrix intersections, and the blue square on a p -directed saddle flow. The quantum-displacement of the vortices near the potential minima, towards the center, is clearly visible.

and the stronger the resulting flow cancellation. Thus tunnelling can be described as a phase space transport phenomenon that plays out over large parts of quantum phase space [20], frustrated through interference in phase space.

For a low energy state, such as Ψ , the positions of remnant vortices originating from the potential's minima positions are quantum-displaced inward, towards the potential barrier, Figs. 3 and 4. Different pictures emerge for other potentials [21] or systems in states more highly excited than Ψ . Remnants of classical stagnation points can get substituted by more than one point each [21] and the overall flow pattern sensitively depends on the choice of state [21].

The occurrence of stagnation points of Wigner flow away from the x -axis ($p \neq 0$) is impossible in classical physics. In the quantum case, even for conservative systems, they can travel long distances in phase space and merge with or split from other stagnation points, Fig. 4.

Their presence alters the topology of phase space flow.

In the case of the Caticha potential in state Ψ , we observe a string of vortices with alternating handedness aligned in the p -direction. They are located near the top of the tunnelling barrier, at position $X_S = -0.258$,

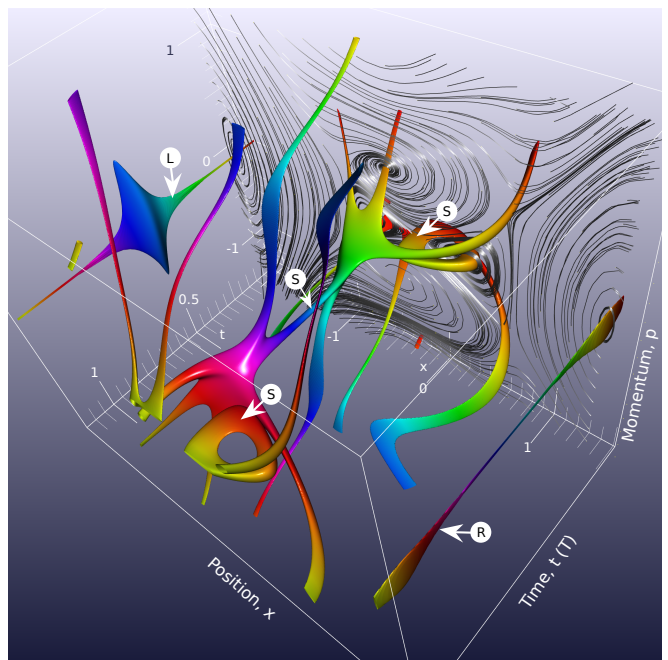


FIG. 4. (color online) Wigner flow's stagnation points' positions across phase space as a function of time. Same parameters as in Fig. 2. The tube surfaces show where in phase space the magnitude of Wigner flow is small $\mathbf{J}(x, p; t)^2 = 3 \cdot 10^{-5}$. They are displayed over 120% of one oscillation period ($t = -0.1 \cdot T \dots 1.1 \cdot T$); the rainbow spectrum is matched to T , red-orange for $t = 0$, via green, cyan at $t = 0.5T$, through blue and purple back to red-orange. Because of the periodicity of the two-state scenario, the red-orange-yellow torus is seen twice at beginning and end of the time window overlap. At the core of all tubes lie time-lines of stagnation points. Their movement through phase space leads to their mergers and splits. The grey flow integration lines are guiding the eye past vortices and separatrices, they do not represent physical flow since they integrate $\mathbf{J}(x, p; t = 0.05)$ at fixed time. The x -coordinate is shown from left well minimum at $X_L = -2.095$ to right well minimum at $X_R = 1.514$, the position of the associated vortices (\textcircled{L} in left well and \textcircled{R} in right), at $p = 0$ and just inside the plot region, confirms the inward quantum-displacement of these stagnation points. The remnant of the classical separatrix stagnation point ($p = 0$, labelled \textcircled{S}) at position $X_S + \delta x_S(t) \approx -0.3$ follows a slightly bent path. It forms the handle of 'Poseidon's green trident', which turns blue as time progresses and then the remnant separatrix stagnation point merges with an incoming counterclockwise vortex in the purple wrist of the four-fingered claw, ceasing to be a separatrix intersection. Shortly after, a separatrix intersection temporarily emerges in conjunction with a vortex to form the torus, subsequently we are 'back to Poseidon's trident'. Mergers or splits are constrained by topological charge [16] conservation.

pinned to the lowest points (in the p -direction) of the Wigner function's interference pattern's meniscus-shaped zero-lines, Fig. 3. Over time they travel downward with the downward movement (in the p -direction) of the interference fringes, Fig. 4. When reaching the x -axis they coalesce with the remnant separatrix intersection point.

Upon their merger the local flow switches to a saddle point's flow pointing in the p -direction, which is impossible in classical phase space, Figs. 1 and 3.

Compared to classical phase portraits, Wigner flow reveals non-classical features and added complexity of quantum phase space dynamics; at the same time it provides, through the conservation of ω , the basis for an analysis of its topological invariants, ordering this complexity. Our numerical findings [18] confirm that winding number conservation applies to isolated stagnation points as well as those that interact with others through splits or mergers, Fig. 4. As an example one can create an integration loop \mathcal{L} around the torus of Fig. 4, since the torus

is formed of a vortex and a separatrix crossing its overall charge is zero, as required given that it appeared out of 'nowhere'.

We conjecture that all stagnation points of the Wigner flow of all superpositions of bound states of non-harmonic potentials carry conserved topological charge [16].

Systems that have been studied using quantum phase space techniques can be analysed using Wigner flow. Such systems arise for example in chemical quantum dynamics [8, 10, 22], 'non-linear' quantum processes in closed single particle [11] or open multi-particle [23–25] systems, classical electromagnetic fields [26] and multi-band semiconductor physics [27].

-
- [1] D. D. Nolte, Phys. Today **63**, 33 (2010).
 - [2] M. V. Berry, in *Am. Inst. Phys. Conf. Ser.*, Vol. 46 (1978) pp. 16–120.
 - [3] E. Wigner, Phys. Rev. **40**, 749 (1932).
 - [4] M. Hillery, R. F. O'Connell, M. O. Scully, and E. P. Wigner, Phys. Rep. **106**, 121 (1984).
 - [5] W. P. Schleich, *Quantum Optics in Phase Space*, by Wolfgang P. Schleich, pp. 716. ISBN 3-527-29435-X. Wiley-VCH, April 2001. (Wiley-VCH, 2001).
 - [6] W. H. Zurek, Nature **412**, 712 (2001), arXiv:quant-ph/0201118.
 - [7] P. Grangier, Science **332**, 313 (2011).
 - [8] A. Donoso and C. C. Martens, Phys. Rev. Lett. **87**, 223202 (2001).
 - [9] H. Bauke and N. R. Itzhak, (2011), arXiv:1101.2683v1.
 - [10] K. H. Hughes, S. M. Parry, G. Parlant, and I. Burghardt, J. Phys. Chem. A **111**, 10269 (2007).
 - [11] O. Gat, J. Phys. A: Math. Theo. **40**, F911 (2007).
 - [12] O. Steuernagel, (2010), arXiv:1008.3929.
 - [13] C. Kurtsiefer, T. Pfau, and J. Mlynek, Nature **386**, 150 (1997).
 - [14] A. Donoso, Y. Zheng, and C. C. Martens, J. Chem. Phys. **119**, 5010 (2003).
 - [15] In degenerate quantum cases flow reversal can occur but none of the other non-classical flow patterns listed here.
 - [16] M. R. Dennis, K. O'Holleran, and M. J. Padgett, in *Progress in Optics*, Vol. 53, edited by E. Wolf (Elsevier, 2009) pp. 293 – 363.
 - [17] A. Caticha, Phys. Rev. A **51**, 4264 (1995).
 - [18] To determine the Wigner functions we integrated y from $-2.7, \dots, 2.7$. The summation cutoff for the determination of J_p was chosen at $l_{max} = 12$.
 - [19] M. V. Berry and N. L. Balazs, J. Phys. A: Math. Gen. **12**, 625 (1979).
 - [20] N. L. Balazs and A. Voros, Ann. Phys. **199**, 123 (1990).
 - [21] Work in preparation.
 - [22] L. L. Gibson, G. C. Schatz, M. A. Ratner, and M. J. Davis, J. Chem. Phys. **86**, 3263 (1987).
 - [23] B. M. Garraway and P. L. Knight, Phys. Rev. A **50**, 2548 (1994).
 - [24] I. Katz, R. Lifshitz, A. Retzker, and R. Straub, N. J. Phys. **10**, 125023 (2008).
 - [25] S. Rips, M. Kiffner, I. Wilson-Rae, and M. J. Hartmann, N. J. Phys. **14**, 023042 (2012).
 - [26] M. Levanda and V. Fleurov, Annals of Physics **292**, 199 (2001), arXiv:cond-mat/0105137.
 - [27] O. Morandi, Phys. Rev. B **80**, 024301 (2009).